ELSEVIER

Contents lists available at ScienceDirect

# Water Research X

journal homepage: www.sciencedirect.com/journal/water-research-x





# Optimization of wet acid phosphorus extraction from sewage sludge ash: Assessment of main influencing factors using an empirical model

Hiep Le 0, Isabell Allwicher, Sarah Müller, David Montag, Thomas Wintgens

Institute of Environmental Engineering (ISA), RWTH Aachen University, Mies-van-der-Rohe-Str. 1 52074 Aachen, Germany

#### ARTICLE INFO

Keywords:
Phosphorus recovery
Sewage sludge ash
Wet acid extraction
Empirical model
Process optimization

#### ABSTRACT

This research investigates the primary factor influencing the phosphorus extraction efficiency (PEE) from incinerated sewage sludge ash (ISSA) using hydrochloric acid (HCl) as the extracting agent. A comprehensive database, comprising both literature and new experimental data, was developed to support the creation of a robust regression model. Based on 152 data sets, this model showed a high coefficient of determination ( $R^2 = 0.86$ ), indicating a solid fit. Key findings revealed that the acid concentration ( $C_{HCl}$ ) had the most significant effect on PEE, followed by the liquid-to-solid ratio (L/S) and contact time (t). The model's predictive accuracy was validated with an  $R^2$  of 0.75 and a Pearson correlation (r) of 0.96, confirming its reliability. The model effectively predicts PEE for ISSA with moderate calcium content (6–12 %) and offers valuable insights into the process, providing guidelines for optimizing the configuration of process parameters. Optimal conditions for achieving high PEE (> 80 %) with acceptable acid costs (0.30–0.35 €/kg  $P_{\text{extracted}}$ ) are expected from an extraction variable (X) of 3.8 and at a moderate  $C_{HCl}$  (3–4 mol/L) & L/S ratio (2–3 L/kg). Still, the model's applicability is limited by the quality of the data, particularly for ashes with high calcium content. Further research is required to expand the database and enhance model accuracy, particularly for optimizing the phosphorus recovery process using wet acid extraction at an industrial scale.

## 1. Introduction

Phosphorus (P) is fundamental for all living organisms, which is not present in its natural elemental form (Pap et al., 2023). The imbalance in resource distribution worldwide not only threatens global P security but also highlights the urgent need for alternative sources (Gorazda et al., 2017). Since 2014, the European Commission has classified phosphate rock as one of the most critical raw materials (EC, 2021). Some European countries (Switzerland, Germany, and Austria) have adopted the obligation to recover P from sewage sludge.

Recently, the EU Commission adopted the Urban Wastewater Treatment Directive (UWWTD), which tightened the effluent concentration of total P (0.5 mg/L) to prevent eutrophication for sensitive water bodies (Boniardi et al., 2024; Pap et al., 2023; Zhao et al., 2024). This will increase P's presence in sewage sludge, which offers a secondary source with consistent quantity. The decline in sludge utilization in agriculture for various reasons led to an increased application of sewage sludges for thermal treatment (Quist-Jensen et al., 2018). Besides, directly recovering P from sewage sludge has been considered

difficult (Yang et al., 2023).

The advantages of higher P content in incinerated sewage sludge ash (ISSA) by up to 13 % and lower treatment volume have led to the recent development of several technologies from ISSA (Boniardi et al., 2022, 2021). Most of them are based on wet acid extraction, where P is extracted from ISSA using highly concentrated mineral acids and then purified from other contaminants. The end product can be phosphoric acid or calcium phosphate, which can be potentially marketed in a wide range of industries, including the fertilizer industry. It is essential to mention that these processes are required, on the one hand, to meet a specific minimum efficiency for P recovery of at least 80 % (BfJ, 2017). On the other hand, if the process is intended for direct use as fertilizer, the resulting product must also comply with the limits set out in the Fertilizer Ordinance concerning heavy metal content (BfJ, 2012). Due to these legal requirements, the extraction stage is crucial as it massively affects the subsequent stages in the P recovery process. Consequently, the optimal trade-off must be identified between high P extraction, low (heavy) metal co-extraction, and minimized operational costs (Luyckx et al., 2021).

E-mail address: wintgens@isa.rwth-aachen.de (T. Wintgens).

<sup>\*</sup> Corresponding author.

In the last decade, there has been a significant increase in the number of studies conducted on the wet acid P extraction process from ISSA on a laboratory scale. Generally, the phosphorus extraction efficiency (PEE,  $M_{P,\ extracted}/M_{P,\ ISSA}$ ) shows a positive correlation with the mentioned extraction parameters since it can be enhanced by raising acid concentration (Cacid), liquid-solid ratio (L/S), contact time (t), or temperature (Biswas et al., 2009; Luyckx et al., 2020; Stark et al., 2006). Authors from different publications obtained that a PEE >85% can just be achieved once Cacid is raised high enough (pH < 2) to dissolve both Ca-and Al-phosphates (Biswas et al., 2009; Luyckx and van Caneghem, 2021). The PEE also increased faster at a higher Cacid. (Biswas et al., 2009) observed a synergy effect on the PEE between Cacid and L/S.

In addition to the process parameter, the PEE is also reported to be ash-specific and depends on the ash composition (Boniardi et al., 2024; Luyckx and van Caneghem, 2021; Luyckx et al., 2020). For instance, a high alkaline mineral buffer in the ash can lead to a higher acid demand since salts and oxides of  $Mg^{2+}$  and  $Ca^{2+}$  interfere with P release (Boniardi et al., 2024; Xu et al., 2023). The sewage sludge combustion at a suitable temperature promotes the formation of the hematite (Fe<sub>2</sub>O<sub>3</sub>) phase in the ISSA, enabling the selective extraction of P compounds (Gorazda et al., 2012, 2016; Li et al., 2018). In contrast, a higher whitlockite (Ca<sub>9</sub>(Mg, Fe)(PO<sub>4</sub>)<sub>6</sub>(PO<sub>3</sub>OH)) content in ISSA has been shown to promote the PEE since P is quickly dissolved by the acid (Herr, 2020; Kleemann et al., 2017; Le Fang et al., 2018).

The literature data on extraction are heterogeneous and incomplete, which makes the analysis of the synergies of different factors extremely challenging. A promising approach has been carried out by (Boniardi et al., 2024) with Design of Experiments. However, to the best of the author's knowledge, a universal mathematical model developed using a database with results from various publications that consider both ash composition and process parameters for PEE prediction has not been available until now. Hence, the overall objective of this comprehensive study is to close this gap by:

 Developing a regression analysis model to quantitatively assess the impact of each main process parameter (C<sub>Acid</sub>, L/S, t) and main elements (Fe, Al, Ca) on the PEE.

- Determining a universal mathematical formula to describe and predict the PEE in the extraction process for various kinds of ISSA.
- Proving a tool to optimize the settings of parameters to fulfill the legal requirement by reaching a defined PEE with high certainty and lower process costs.

#### 2. Results and discussion

## 2.1. Experimental results

Fig. 1 illustrates the author's extraction tests PEE in response to different process configurations regarding the CHCI, t, and L/S of different ashes. It was observed that the PEE increased for higher CHCI and longer t. When the CHCl was below 2 mol/L, achieving a target PEE above 80 % proved challenging. Conversely, most leaching tests could reach this target at a CHCI greater than 2.4 mol/L. This outcome confirmed the observation by (Luyckx and van Caneghem, 2021; Esposito et al., 2024) that a particularly high acid concentration is required for efficient extraction, regardless of the L/S. However, it was also noted that the PEE remained below 70 % in some experiments, even at a high  $C_{HCl}$  over 4 mol/L. The variation of the PEE at L/S ratio (L/S= 3) can be explained by the reaction of the different ash properties with the contact time. Hence, the ash characteristic is likely to influence the PEE substantially, in addition to the process configuration. On the other hand, the impact of a higher L/S = 10 remains unclear due to the low PEE. Perhaps the superimposing phenomenon with different impact factors could be a reason. The developed modeling result should address this aspect and provide a more comprehensive interpretation of the observed experimental results.

## 2.2. Modeling results

#### 2.2.1. Model #1

Fig. 2 illustrates the modeling result for Model #1. For exponents of the parameters  $e_{L/S}$  and  $e_{HCL}$  below  $e_t=1$ , the model showed a bad fit to the data with a low determination coefficient ( $R^2$ ), which could be observed with the blue color in this area. A higher value of  $e_{L/S}$  and  $e_{HCL}$  between 2.5 and 3.5 enhanced  $R^2$ , which is evident in the more

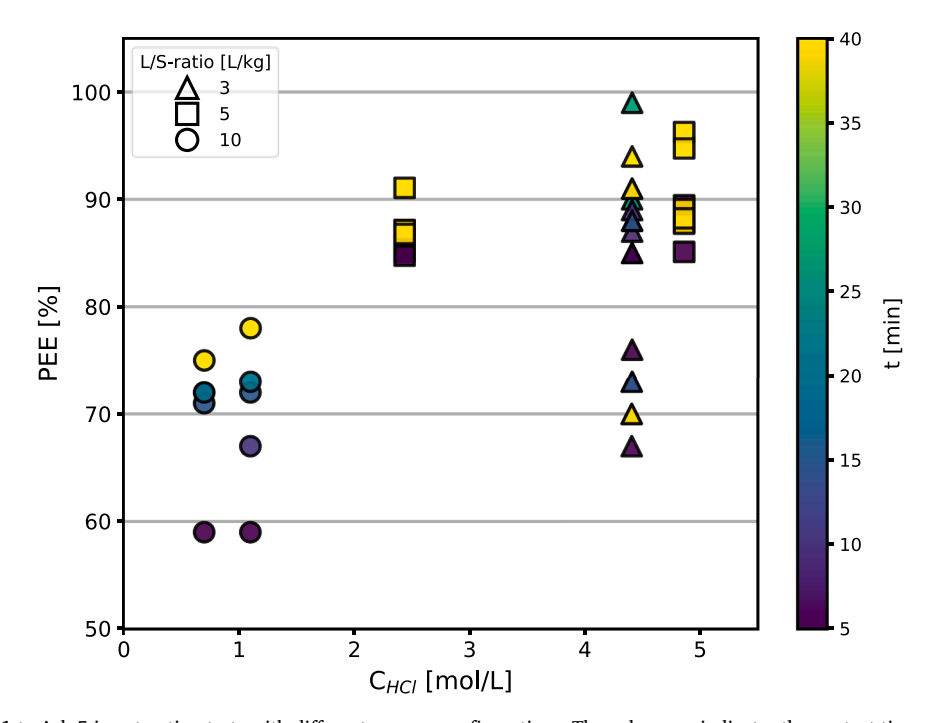


Fig. 1. PEE results of Ash 1 to Ash 5 in extraction tests with different process configurations. The color map indicates the contact time, while the markers illustrate different L/S ratios.

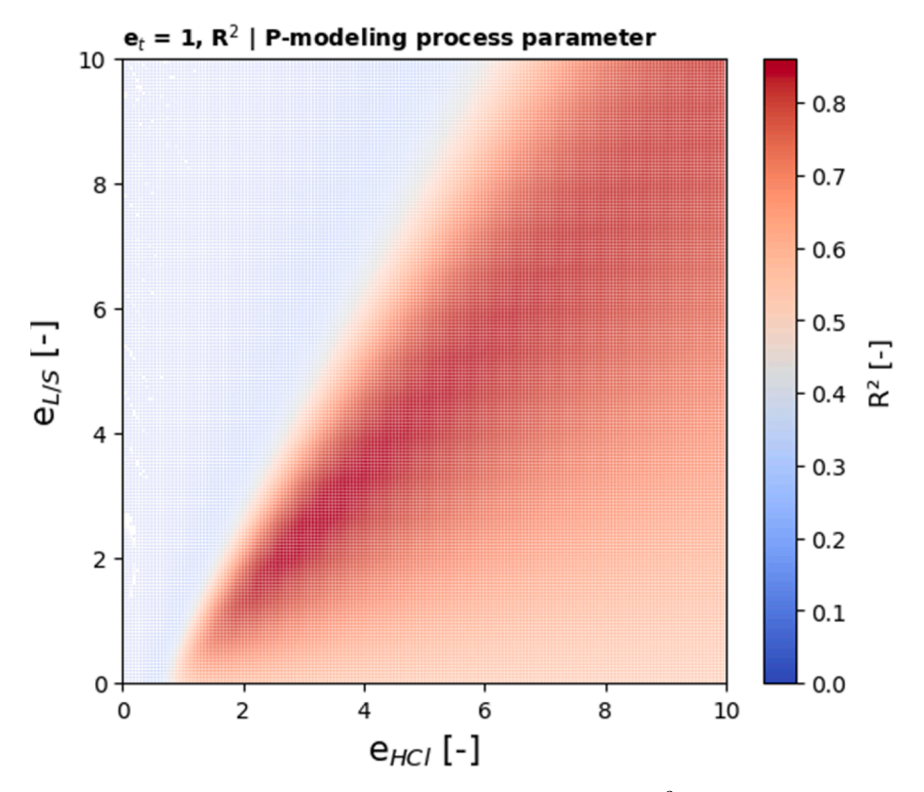


Fig. 2. Heatmap showing results of Model #1. The color map indicates the determination of coefficient  $R^2$  for each pair of  $e_{HCl}$  on the x-axis and  $e_{L/S}$  on the y-axis, varied between 0 and 10.

significant influence of  $C_{HCl}$  and L/S on the PEE than t. The exponents in this range provided optimal results, characterized by the dark red area in the figure with the highest  $R^2$  coefficient and the lowest deviation

(RMSE). A further increase in the exponents up to 10 did not yield any additional improvement to the model. The best combination of exponents was obtained at  $e_{HCl}=3.1$  and  $e_{L/S}=2.5$ . This led to the finding

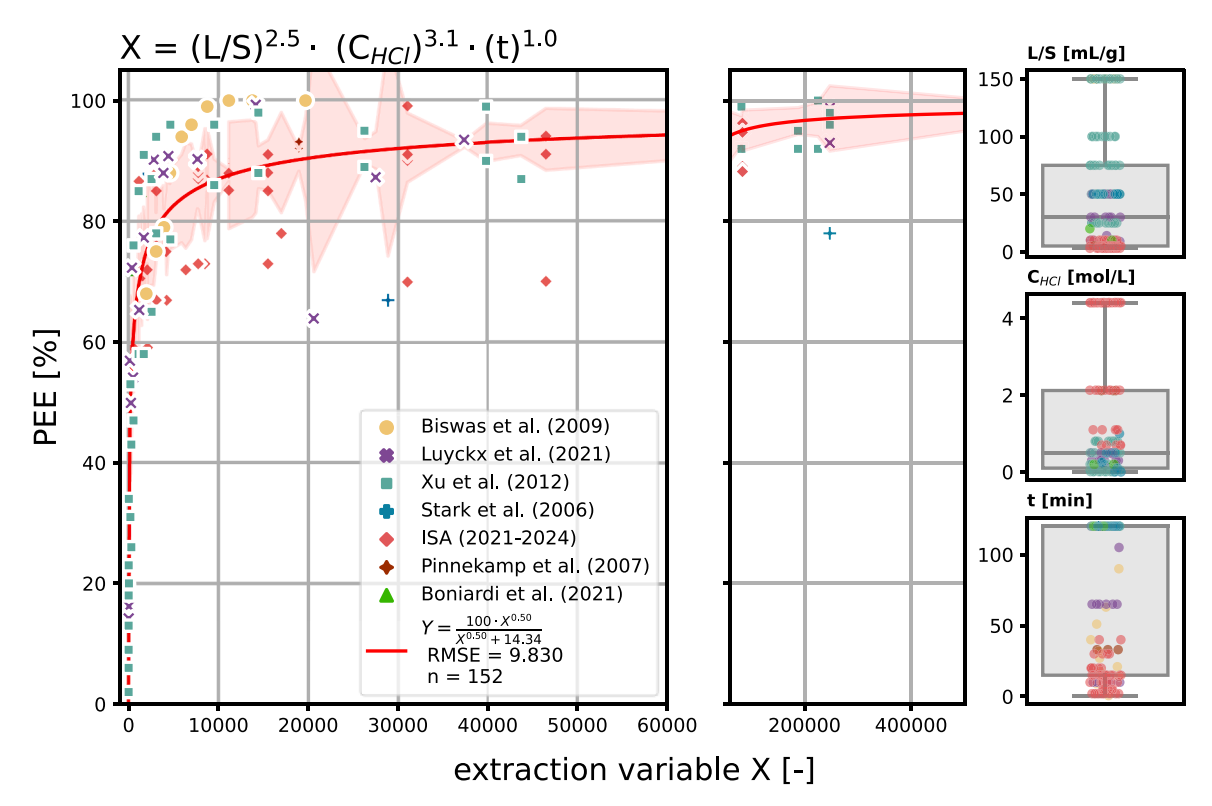


Fig. 3. PEE curve function of Model #1. The curve shows the trendline after regression analysis using 152 datasets from the database ( $R^2 = 0.86$ ). The points are explicitly marked according to their publication of origin. The shaded area demonstrates the mean deviation of the prediction PEE from the observed PEE. Three boxplots on the right side represent the range of process parameters L/S,  $C_{HCl}$ , and t considered in this model.

that the acid concentration  $C_{HCl}$  had the most significant impact on the PEE. In other words, varying  $C_{HCl}$  could induce the most critical change in the PEE.

The optimum variables a and b were determined using regression analysis as 0.5 and 14.34, respectively. Therefore, the function employed Y = f(X) using extraction variable X to predict the PEE can be defined as follows:

$$X = \left(L/S\right)^{2.5} * \left(C_{HCl}\right)^{3.1} * t^{1.0}$$

$$Y = f(X) = \frac{X^{0.5}}{X^{0.5} + 14.34}$$

Fig. 3 illustrates the PEE curve function (Y). The curve demonstrated a strong correlation between the predicted P extraction efficiency (PEE<sub>pred</sub>) and the observed data from different literature (PEE<sub>obs</sub>), proved by a high Pearson correlation (r=0.93,  $p=2\times10^{-67}$ ).

The PEE rapidly increased in the lower range of X and reached a plateau of around 90 % at approximately X=10,000, where it underwent only a minor adjustment towards 100 % extraction efficiency. These observations indicate that the variation in process parameters has reached its limits, beyond which higher  $c_{HCL}$  or L/S no longer significantly enhance the PEE. The remaining 10 % of P is likely to be firmly bound in calcium or iron compounds like hematite and thus cannot be dissolved, as (Gorazda et al., 2016) described. The markedly lower PEE (< 80 %) observed in some data, despite X exceeding 20,000, can be attributed to the specific composition of the respective ash used, which was not yet considered in Model #1. Besides, it is crucial to mention that Model #1 performed optimally for ashes and processes with parameters in the range used for the simulation. Overall, Model #1 demonstrated a good level of performance, with a strong correlation between the predicted PEE and the observed values ( $R^2=0.86$ , n=152).

## 2.2.2. Model #2

Model #2 incorporates 62 data sets, considering the concentrations of predominant elements (P, Al, Fe, and Ca) in the ash, which represent the most common phosphate compounds (Meng et al., 2019). Since the data is more limited than for a model without ash components, the  $\mathbb{R}^2$  of Model #1 deteriorated to 0.78 before the ash parameters were integrated.

The modeling results are depicted in Figure A1 in the Supplementary Material (SM). It could be observed that as the exponents of the ash parameter decrease, the R<sup>2</sup> value increases. This result indicated that the ash composition did not affect the PEE significantly as the process parameters did. Nevertheless, a slight improvement of R2 was observed when  $e_{P/Fe} = 0.2$  ( $R^2 = 0.8$ , Figure A2 in SM). A high content of Fe and a low P/Fe ratio would prevent a small fraction of P from being extracted. For instance, it could be due to the appearance of the hematite phase in the ash, which was observed to be responsible for the selective extraction of the P compound (Gorazda et al., 2017, 2016). Regarding the P/Ca and the P/Al ratio, the effect of those elements on the PEE was not strong enough to be detected by Model #2. This is, on the one hand, due to the limited data set. On the other hand, the ranges of P/Ca and P/Al ratios (0.6-1.5 and 0.7-2, respectively) appeared to have a narrow variation due to the lack of different ash qualities. Nevertheless, the mean deviation between the predicted PEE and the observed PEE was reduced to RMSE = 9.2. The function of the extraction variable (X) and the extraction curve (Y) of Model #2 was defined as:

$$X = \left( L/S \right)^{2.5} * \left( C_{HCl} \right)^{3.1} * t^{1.0} * \left( P/Fe \right)^{0.2}$$

$$Y = f(X) = \frac{X^{0.52}}{X^{0.52} + 16.23}$$

Figure A3 in SM shows the changing of predicted PEE with a variation of each parameter per time. The slope of the line becomes steeper as the exponent of the parameters increases. The steep slope of  $C_{HCl}$ 

confirmed its most decisive influence on the PEE, which was also stated by (Boniardi et al., 2024).  $C_{HCl}$  is the main factor driving the extraction process. PEE rose sharply, over 80 % when  $C_{HCl}$  exceeded 2.5 mol/L. From  $C_{HCl}=3$  mol/L onwards, the PEE increased much slower until it reached 90 %. Furthermore, it is advantageous to vary the L/S ratio between 2 and 5 to achieve a higher PEE. In contrast, the contact time (t) shows significantly less impact on the PEE. For the P/Fe ratio, the PEE stays stable across varied ranges (0.5–2.5).

#### 2.3. Model validation

Owing to an extensive data set of different ISSA and a more robust determination coefficient, Model#1 was chosen for validation. The validation was carried out using the same configuration of process parameters ( $C_{HCl}$ , L/S, t) and comparing the PEE<sub>pred</sub> with the experiment results (PEE<sub>obs</sub>) specified in (Boniardi et al., 2024). The main difference between the two ISSA investigated in (Boniardi et al., 2024) was Ca-content, which was 21.8 % in the Ca-rich ash (ISSA<sub>Bon,Ca+</sub>) and 12.5 % in the other (ISSA<sub>Bon,Ca</sub>.). Fig. 4 depicts the validation result of Model #1 in this study using the second ash (ISSA<sub>Bon,Ca</sub>.), compared to other models (Bon#3 and Bon#4) developed by (Boniardi et al., 2024).

It can be stated that Model#1 of this study (in red) generally predicted the PEE higher than the observed one (Fig. 4, PEE<sub>obs</sub>, in blue). However, the results in the higher range of PEE showed high accuracy and fitted the data well. Indeed, test runs with PEE exceeding the 80 % extraction target could be determined correctly. In the lower range of PEE <50%, Model Bon#3 seemed to perform better than Model #1 but struggled in the range of PEE between 50 % and 80 % due to underestimation. Model Bon#4 best fits ISSABon,Ca- with a high  $R^2$  of 0.98 and an RMSE of 0.3. In a nutshell, Model #1 showed valid results and a good fit with the experimental results ( $R^2=0.75,\,RMSE=13.6$ ). The model's robustness is expected to be as good as Bon#3.

However, Model#1 exhibited suboptimal fitting with the experimental data when confronted with Ca-rich ash (ISSA $_{Bon,Ca+}$ ). The PEE $_{pred}$  was systematically higher than the PEE $_{obs}$  (see Figure A4 in SM), suggesting that Model #1 could not explain all the variability, possibly due to the missing parameter of Ca-content and the alkalinity, which is responsible for the selective P extraction. It was also reported that further ash characteristics, like particle size, could affect the PEE due to the different contact surface area with the extractant acid (Liu et al., 2023; Herr, 2020). Indeed, once further data are available, the overestimated PEE $_{obs}$ , especially if alkalinity or further ash characteristics were considered.

Besides, the models developed in this study strongly depend on the range of the ash compositions and process conditions available in the earlier studies, since a prediction outside the range of the parameter can decrease the prediction's reliability (Boniardi et al., 2024). With respect to the work of (Boniardi et al., 2024), the ISSABon,Ca+ and ISSABon,Ca- used showed significantly higher Ca contents than other ashes reported in the literature (6- 12 % Ca) (Abis et al., 2018; Schaum, 2007; Sichler et al., 2022). Consequently, it is hardly surprising that Model #1 performed sub-optimally on the ISSABon,Ca+ with 28 % Ca (see Figure A4). These findings can be confirmed by the fact that Model #1 worked well with the ISSABon,Ca-, which still had a comparatively high Ca content (12.5 %) but demonstrated a substantial proximity to the modeled range.

In summary, Model #1 validly predicted the PEE for ashes with moderate Ca content (6–12%). Model #1 is expected to achieve a better fit using a representative database that considers wider ranges of Ca concentration in the ash. This is fundamental since further ash parameters can be simultaneously integrated into the model, as shown in Model #2.

H. Le et al. Water Research X 29 (2025) 100352

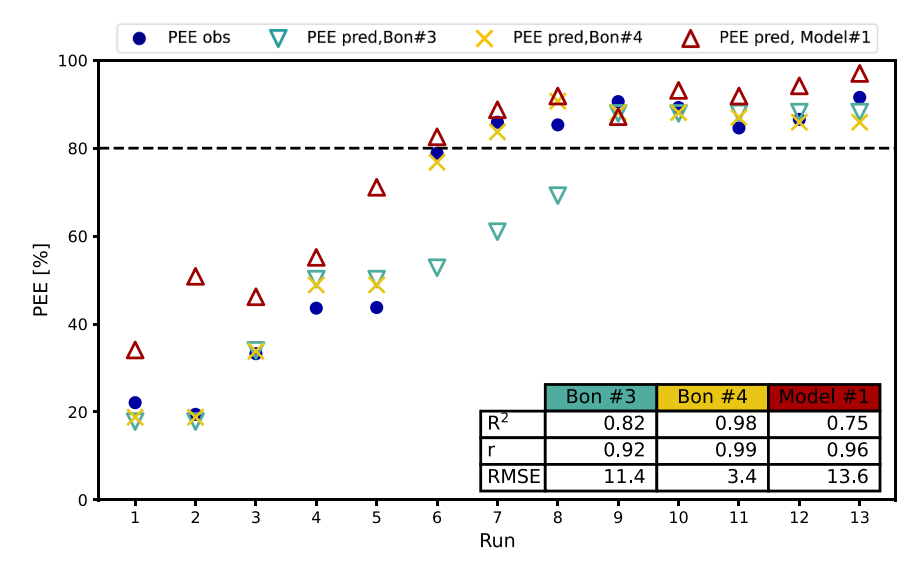


Fig. 4. Validation of Model #1 with ISSA<sub>Bon,Ca</sub>. compared to other models (Bon #3 and Bon #4). The table shows statistical values, indicating the robustness of each model: coefficient of determination (R<sup>2</sup>), Pearson correlation (r), and mean deviation (RMSE).

## 2.4. Optimization of the wet extraction process

The extraction variable (X) of predictive model can be used to design the process's initial parameter settings and to optimize the acid costs by considering the interaction and synergies of extraction parameters. It aimed to minimize the acid demand while keeping the PPE high. The regression curve of Model #1 is depicted in Figure A5 (in SM) in logarithmic form for better visualization. As mentioned above, a PEE >80 % must be achieved to comply with the legal requirements in Germany. Considering the statistical T-test, a confidence interval of over 95 % (p < 0.05) can be guaranteed when X is chosen to be 3.8  $\pm$  0.1, giving a PEE

$$= 86.6 \pm 6.5 (n = 9).$$

Fig. 5 illustrates the cost of acid demand calculated for different combinations of  $C_{HCl}$  and L/S, referring to the amount of extracted phosphorus ( $P_{\text{extracted}}$ ). The contact time was set to 20 min, while the price of commercial HCl (35 %) was conservatively assumed to be 210  $\epsilon$ /MT (Chemanalyst, 2024; Chen et al., 2024). The PEE<sub>predicted</sub> was determined using Model #1, while the P content in the ash was deemed to be 7 %. Thus, the relative cost could be calculated using the following equation:

$$Cost\,HCl,\,\,relative\,\,[\textit{$\epsilon$}\,/\,\,kg\,\,Pextracted] = \frac{C_{HCl}\,\,[mol/L]*L\big/S\,[L/kg]*\,\,\textit{$M_{HCl}[g/mol]*$}\,\,\textit{$P_{HCl,com}[\epsilon/MT]$} *10^{-3}}{C_{HCl,com}\,\,[\%]} *\,\,PEE_{pred}\,\,[\%]$$

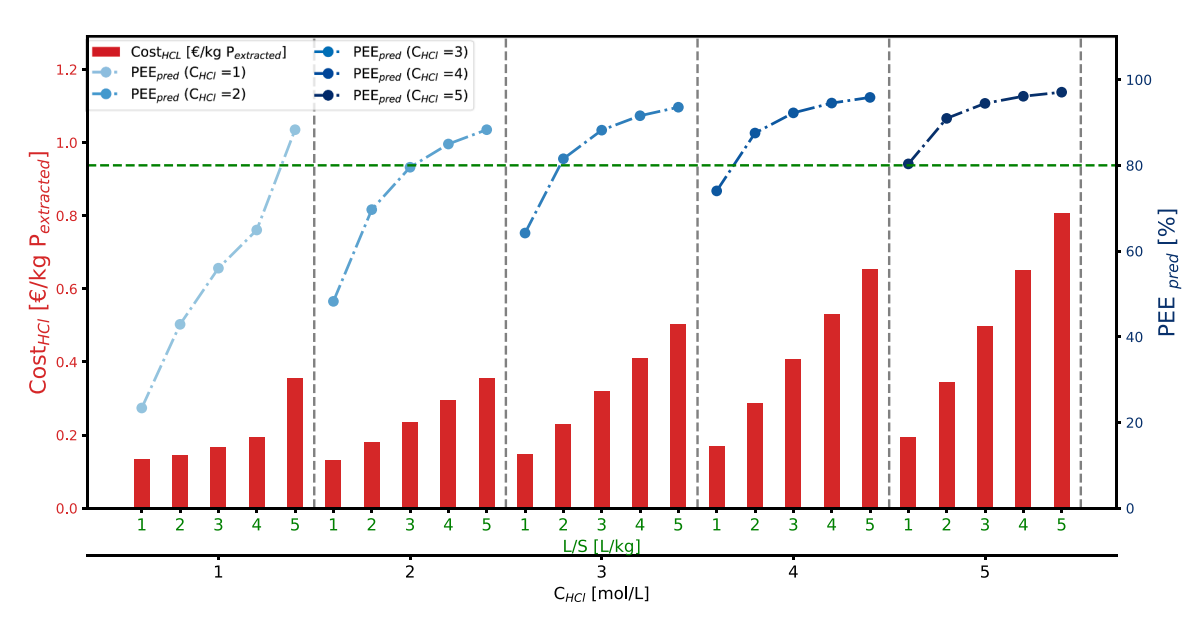


Fig. 5. Actual cost of acid demand per kg extracted phosphorus. The x-axis indicates the combination of process parameters of  $C_{HCl}$  and L/S. The blue y-axis on the right side indicates the predicted PEE with Model #1, while the relative acid cost is illustrated in red bars, which belong to the y-axis in red on the left. The dashed lines of PEE are only to guide the readers' eyes.

As shown in Fig. 5, the desired PEE (> 80 %) at a low  $C_{HCI}$  range (1–2 mol/L) was only obtained by setting a high L/S of at least 5 L/kg. The relative acid cost required for this condition was approximately 0.35-0.4  $\epsilon$ /kg  $P_{extracted}$ . In contrast, for higher  $C_{HCI}$ , increasing L/S is deemed unnecessary as the PEE enhancement was no longer significant. Besides, increased demand for acid results in a rapid escalation of the relative acid cost to 0.7-0.8  $\epsilon$ /kg  $P_{extracted}$  or 3–4 kgHCI/kg  $P_{extracted}$ . According to a recent publication by (Esposito et al., 2024), the acid demand for P extraction from ISSA on the laboratory scale is currently between 5–10 kgHCI/kg  $P_{extracted}$ , indicating a potential for optimization using the developed model in this study. Consequently, the optimum result was recorded at a moderate range of  $C_{HCL}$  and L/S (4 mol/L and 2 L/kg or 3 mol/L and 3 L/kg). These test conditions are expected to securely achieve a PEE over 85 %, while the relative costs were maintained at a low level, around 0.30 - 0.35  $\epsilon$ /kg  $P_{extracted}$ .

## 3. Conclusion

This research investigated the main influences on the phosphorus extraction efficiency (PEE) from incinerated sewage sludge ash (ISSA), using HCl as the extracting agent. The modeling results confirmed the observation in the previous studies that the acid concentration impacts the PEE most significantly, followed by the L/S and t (n=152,  $R^2=0.86$ ). Predictive Model #1 showed good accuracy in predicting the PEE ( $R^2=0.75$ , r=0.96) after being validated with ISSA from other publications. An extraction variable (X) higher than 3.8 is recommended to achieve a PEE over 80 % (p<0.05). Predictive Model #2 considered further ash characteristics and offered the opportunity to assess other non-process parameters using the same method.

However, this empirical approach to assessing the PEE still has limitations since its applicability strongly depends on the quality of the database. It is evident that as the ash composition deviates further from the database's range. The model's accuracy undergoes a corresponding decline for ashes with exceptionally high Ca content (> 15 %) since the alkalinity remains a decisive parameter for the process. Nevertheless, for ISSA with moderate Ca-content (6-12 %), predictive Model #1 could validly predict the PEE<sub>pred</sub> and provide a helpful orientation tool to configure the process parameters. A moderate L/S and CHCl (2-4 L/kg and 3-5 mol/L, respectively) are recommended to achieve the requirement of PEE > 80 % as part of the German P-recovery strategy without rapidly increasing the acid costs (0.30 - 0.35 €/kg P<sub>extracted</sub>). In the next step, the predictive models will continue to be expanded and validated on the basis of data in further research with more ash parameters. The transferability of predictive models in the case of upscaling will also be assessed by applying them to an extraction pilot plant on an industrial scale, which processes up to 1000 t ISSA/a in Germany.

#### 4. Material and methods

#### 4.1. Sewage sludge ash sample

For this study, five sewage sludge ashes from different monoincineration plants in Germany were obtained for analysis. Table A1 in SM presents an overview of ash composition with the concentration of dominant elements. The P concentration varied between 6 and 10 wt.-%, which was within the typical range reported in the ISSA database for municipal WWTPs in Germany (Petzet et al., 2012; Sichler et al., 2022).

Ash 4 and Ash 5 showed higher alkalinity, with higher Mg<sup>2+</sup> and Ca<sup>2+</sup> concentrations than the initial three ashes. Ash 1 and Ash 2 had a higher Fe content, respectively, attributed to the P precipitation with Fesalts. In contrast, Ash 5 was derived from sewage sludge with Al-salt used as a precipitation agent. By selecting ashes with diverse properties and origins, a model could be developed to cover a broad spectrum of ash characteristics.

#### 4.2. Phosphorus wet acid extraction

Samples of ISSA were added to hydrochloric acid (HCl) at a certain L/S ratio (3- 10 mL/g) and acid concentration (0.7- 4.4 mol/L) in a 600 mL beaker. The solution was stirred continuously on a magnetic stirring plate (IKAMAC®, model RTC) at 350 rpm. A specific contact time (2 – 40 min) was set during extraction. The suspension was then filtered through a 0.45  $\mu$ m membrane filter (Macherey-Nagel, PORAFIL® CM), and the filtrate was analyzed using ICP OES (PerkinElmer 5300 DV) and ICP MS (Agilent 7700) based on DIN EN 16,170:2017–01 and DIN EN 16,171:2017–01, respectively.

#### 4.3. Database design

The data used in this study are based on extraction results with hydrochloric acid from 7 publications between 2006 and 2021 supplemented by the author's own research from 2021 to 2024. Due to the large and heterogeneous database, the model considered the extraction at a temperature  $<50\,^{\circ}\text{C}$  and a contact time <120 min. These specifications are deemed reasonable and realistic, especially concerning an upscaling of the process to an industrial scale.

The availability of data, sorted by literature, is summarized in Figure A6 in SM. As illustrated, the database includes results from 152 experiments with details about the extraction process parameters and the PEE. However, only 62 experimental datasets provided the composition of the ISSA used, which is necessary for modeling. Generally, the effect parameters can be classified into two groups:

- Process parameters: L/S-ratio (L/S), acid concentration (C<sub>HCl</sub>), contact time (t)
- Ash parameters: concentration of dominant elements Al, Fe, Ca, and P

These data sets are decisive and specific for the models developed in this work, which will be introduced in the following part of this study. For the best validation of the developed models, ash composition and experimental results introduced in the most current publication of (Boniardi et al., 2024) were used.

## 4.4. Modeling and regression analysis

## 4.4.1. Modeling approach

Fig. 6 shows a flow chart summarizing the modeling approach: Each parameter  $(P_n)$  was assigned an exponent  $(e_n)$ , indicating the strength of the parameter's influence on the extraction efficiency. An extraction variable (X) (see Fig. 6\*) was defined by the multiplication of every parameter  $(P_n)$  considered in the model with its exponent  $(e_n)$ :

$$X = (P_1)^{e1} * (P_2)^{e2} * (P_3)^{e3} * \dots * (P_n)^{en}$$

The value of one random exponent was set to 1 as baseline, while the other exponents were varied in specific increments from 0 to 10. As indicated in previous publications, the PEE is expected to increase rapidly at the beginning and then reach a plateau. Therefore, the Michaelis-Menten equation is expected to describe the PEE (Y) with unknown variables a and b (see Fig. 6\*\*).

An iterative procedure was carried out to perform a regression analysis of the extraction variable (X) and the PEE (Y). The exponents  $e_n$  of each parameter  $P_n$  were optimized. After the modeling, the exponents' combination with the lowest root mean square error (RMSE) and highest coefficient determination  $(R^2)$  was considered the optimum result for the extraction variable (X).  $R^2$  is a statistical coefficient that shows the model's strength and the predicted value's fitting. At the same time, RMSE indicates the mean deviation of the model in comparison to the observed result.  $R^2$  and RMSE can be calculated as follows:

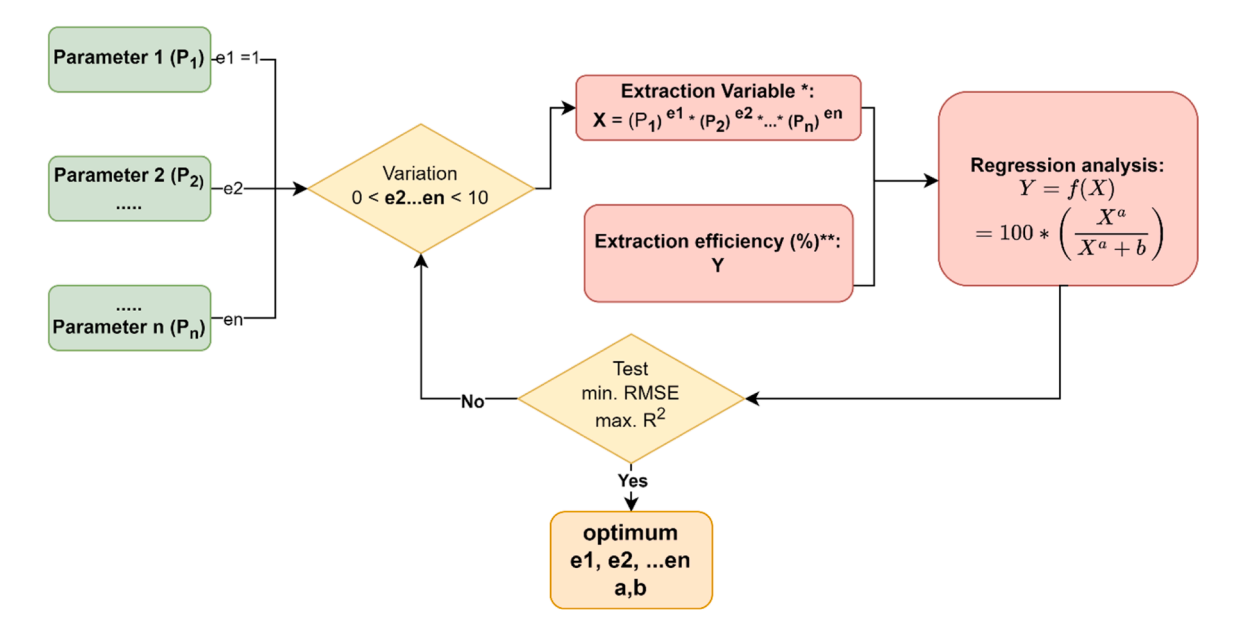


Fig. 6. Flow chart with an overview of the modeling scheme.

$$\textit{RMSE} = \sqrt{\frac{\sum_{i} \left(\textit{PEE}, i - f(\textit{Xi})\right)^{2}}{i}}$$

$$R^{2} = \frac{\sum_{i} (f(Xi) - PEE, mean)^{2}}{\sum_{i} (PEE, i - PEE, mean)^{2}}$$

The extraction curve function f(X), determined with the variables a and b, was used as the final function to predict PEE. The modeling was carried out using Python 3.9.13.

## 4.4.2. Configuration of models

Since the P-concentration varied between the different ISSA, the proportion of P concentration to one of each dominant element ( $C_{Phos-phorus}[mg/kg]/C_{Element}$  [mg/kg]) will be considered as input in the model for a uniform comparison. Based on the results of earlier studies, the first group of the mentioned effect parameters seemed to have a decisive influence on the PEE. Thus, the first model (**Model #1**) only included the process parameters (Figure A6). The exponent of contact time was set to 1 (e<sub>t</sub> =1) as a baseline. The other parameters would impact the PEE more if their exponents exceeded this value. The exponents for  $C_{HCl}$  and L/S were varied from 0 to 10 in increments of 0.1. There are 152 data sets available to feed Model #1.

**Model #2** additionally considered the ash composition and most relevant P-compounds in the ISSA (calcium-, iron- and aluminium phosphate) with 62 data sets. Since heavy metals don't have such a high content in the ash and can be clarified in further process stages with electrodialysis or sulphide precipitation, their impact on the PEE is expected to be limited and hence not included in the modeling.

Based on the developed Model #1, the optimal exponents for process parameters were directly applied. The exponents for ash parameters ranged between 0 and 10. In contrast to Model #1 a higher increment (estep = 0.2) was chosen to limit the increase in simulation steps from 40,000 to just 162,500. The main details of both models are summarized in Table A2 in SM.

## CRediT authorship contribution statement

**Hiep Le:** Writing – original draft, Visualization, Investigation, Formal analysis, Data curation, Conceptualization. **Isabell Allwicher:** Investigation, Data curation. **Sarah Müller:** Writing – review & editing,

Investigation. **David Montag:** Writing – review & editing, Supervision, Project administration, Funding acquisition. **Thomas Wintgens:** Writing – review & editing, Supervision, Funding acquisition.

#### **Declaration of competing interest**

The authors declare the following financial interests/personal relationships which may be considered as potential competing interests:

Thomas Wintgens reports financial support was provided by Federal Ministry of Education and Research of Germany (Project AMPHORE, grant number: 02WPR1543I). If there are other authors, they declare that they have no known competing financial interests or personal relationships that could have appeared to influence the work reported in this paper.

## Supplementary materials

Supplementary material associated with this article can be found, in the online version, at doi:10.1016/j.wroa.2025.100352.

## Data availability

Data will be made available on request

#### References

Abis, M., Calmano, W., Kuchta, K., 2018. Innovative technologies for phosphorus recovery from sewage sludge Ash. Detritus 1, 23–29.

BfJ (2017) 'Sewage sludge Ordinance- abfallklärsschlammverordnung-verordnung über die verwertung von Klärschlamm, Klärschlammgemisch und Klärschlammkompost (Klärschlammverordnung - AbfKlärV)' [online] https://www.gesetze-im-internet. de/abfkl\_rv\_2017/AbfKl%C3%A4rV.pdf (Accessed 28 July 2024).

BfJ (2012) 'Fertilzer Ordinance- verordnung über das Inverkehrbringen von Düngemitteln, Bodenhilfsstoffen, Kultursubstraten und Pflanzenhilfsmitteln (Düngemittelverordnung - DüMV' [online] https://www.gesetze-im-internet.de/d\_mv\_2012/D%C3%BCMV.pdf (Accessed 28 July 2024).

Biswas, B.K., Inoue, K., Harada, H., Ohto, K., Kawakita, H., 2009. Leaching of phosphorus from incinerated sewage sludge ash by means of acid extraction followed by adsorption on orange waste gel. J. Environ. Sci. (China) 21 (12), 1753–1760.

Boniardi, G., Paini, E., Seljak, T., Azzellino, A., Volonterio, A., Canziani, R., Turolla, A., 2024. Optimization of phosphorus wet acid extraction from sewage sludge ashes: detailed process insight via multi-variate statistical techniques. J. Clean Prod. 458, 142491.

- Boniardi, G., Turolla, A., Fiameni, L., Gelmi, E., Bontempi, E., Canziani, R., 2022. Phosphorus recovery from a pilot-scale grate furnace: influencing factors beyond wet chemical leaching conditions. J. Int. Associat. Water Pollut. Res. 85 (9), 2525–2538.
- Boniardi, G., Turolla, A., Fiameni, L., Gelmi, E., Malpei, F., Bontempi, E., Canziani, R., 2021. Assessment of a simple and replicable procedure for selective phosphorus recovery from sewage sludge ashes by wet chemical extraction and precipitation. Chemosphere 285, 131476.
- Chemanalyst (2024) 'Hydrochloric acid price trend and forecast' [online] https://www.chemanalyst.com/Pricing-data/hydrochloric-acid-61 (Accessed 4 December 2024).
- Chen, C., Wang, L., Xu, Y., Wang, F., 2024. Production of hydroxyapatite utilizing calcium and phosphorus in sewage sludge incineration ash. Process Safet. Environ. Protect. 191, 2513–2521.
- EC (2021) 'Critical raw materials resilience: charting a path towards greater security and sustainability'.
- Esposito, L., Boniardi, G., Frigerio, M., Guembe, M., García-Zubiri, Í.X., El Chami, D., Canziani, R., Turolla, A., 2024. Development of a multi-objective support tool for optimizing phosphorus recovery from sewage sludge ash: a step towards process feasibility. J. Clean Prod. 485, 144378.
- Gorazda, K., Kowalski, Z., Wzorek, Z., 2012. From sewage sludge ash to calcium phosphate fertilizers. Polish J. Chemic. Techn. 14 (3), 54–58.
- Gorazda, K., Tarko, B., Wzorek, Z., Kominko, H., Nowak, A.K., Kulczycka, J., Henclik, A., Smol, M., 2017. Fertilisers production from ashes after sewage sludge combustion - A strategy towards sustainable development. Environ. Res. 154, 171–180.
- Gorazda, K., Tarko, B., Wzorek, Z., Nowak, A.K., Kulczycka, J., Henclik, A., 2016. Characteristic of wet method of phosphorus recovery from polish sewage sludge ash with nitric acid. Open Chem. 14, 37–45.
- Herr, P. (2020) Untersuchungen zur mitverwertung von Klärschlammaschen bei der nasschemischen phosphorsäureherstellung. Dissertation, Technische Universität München, München.
- Kleemann, R., Chenoweth, J., Clift, R., Morse, S., Pearce, P., Saroj, D., 2017. Comparison of phosphorus recovery from incinerated sewage sludge ash (ISSA) and pyrolysed sewage sludge char (PSSC). Waste Manag. 60, 201–210.
- Le, Fang, Li, J.-S., Guo, M.Z., Cheeseman, C.R., Tsang, D.C.W., Donatello, S., Poon, C.S., 2018. Phosphorus recovery and leaching of trace elements from incinerated sewage sludge ash (ISSA). Chemosphere 193, 278–287.
- Li, J.-S., Chen, Z., Wang, Q.-M., Le, Fang, Xue, Q., Cheeseman, C.R., Donatello, S., Liu, L., Poon, C.S., 2018. Change in re-use value of incinerated sewage sludge ash due to chemical extraction of phosphorus. Waste Manag. 74, 404–412.
- Liu, H., Lyczko, N., Nzihou, A., Eskicioglu, C., 2023. Phosphorus recovery from municipal sludge-derived hydrochar: insights into leaching mechanisms and hydroxyapatite synthesis. Water Res. 241, 120138.
- Luyckx, L., Geerts, S., van Caneghem, J., 2020. Closing the phosphorus cycle: multicriteria techno-economic optimization of phosphorus extraction from wastewater treatment sludge ash. Sci. Total Environ. 713, 135543.

- Luyckx, L., Sousa Correia, D.S., van Caneghem, J., 2021. Linking phosphorus extraction from different types of biomass incineration ash to Ash mineralogy, Ash composition and chemical characteristics of various types of extraction liquids. Waste Biomass Valoriz. 12 (9), 5235–5248.
- Luyckx, L., van Caneghem, J., 2021. Recovery of phosphorus from sewage sludge ash: influence of incineration temperature on ash mineralogy and related phosphorus and heavy metal extraction. J. Environ. Chemic. Eng. 9 (6), 106471.
- Meng, X., Huang, Q., Xu, J., Gao, H., Yan, J., 2019. A review of phosphorus recovery from different thermal treatment products of sewage sludge. Waste Dispos. Sustain. Energy 1 (2), 99–115.
- Pap, S., Zhang, H., Bogdan, A., Elsby, D.T., Gibb, S.W., Bremner, B., Taggart, M.A., 2023. Pilot-scale phosphate recovery from wastewater to create a fertiliser product: an integrated assessment of adsorbent performance and quality. Water Res. 228 (Pt B), 110340
- Petzet, S., Peplinski, B., Cornel, P., 2012. On wet chemical phosphorus recovery from sewage sludge ash by acidic or alkaline leaching and an optimized combination of both. Water Res. 46 (12), 3769–3780.
- Quist-Jensen, C.A., Wybrandt, L., Løkkegaard, H., Antonsen, S.B., Jensen, H.C., Nielsen, A.H., Christensen, M.L., 2018. Acidification and recovery of phosphorus from digested and non-digested sludge. Water Res. 146, 307–317.
- Schaum, C.A. (2007) Verfahren für eine zukünftige klärschlammbehandlung. Klärschlammkonditionierung und rückgewinnung von Phosphor aus Klärschlammasche. Dissertation, Technische Universität Darmstadt, Darmstadt.
- Sichler, T.C., Montag, D., Barjenbruch, M., Mauch, T., Sommerfeld, T., Ehm, J.-H., Adam, C., 2022. Variation of the element composition of municipal sewage sludges in the context of new regulations on phosphorus recovery in Germany. Environ. Sci. Europe 34 (1), 84.
- Stark, K., Plaza, E., Hultman, B., 2006. Phosphorus release from ash, dried sludge and sludge residue from supercritical water oxidation by acid or base. Chemosphere 62 (5), 827–832.
- Xu, Y., Zhang, L., Chen, J., Liu, T., Li, N., Xu, J., Yin, W., Li, D., Zhang, Y., Zhou, X., 2023. Phosphorus recovery from sewage sludge ash (SSA): an integrated technical, environmental and economic assessment of wet-chemical and thermochemical methods. J. Environ. Manage. 344, 118691.
- Yang, L., Guo, X., Liang, S., Yang, F., Wen, M., Yuan, S., Xiao, K., Yu, W., Hu, J., Hou, H., Yang, J., 2023. A sustainable strategy for recovery of phosphorus as vivianite from sewage sludge via alkali-activated pyrolysis, water leaching and crystallization. Water Res. 233, 119769.
- Zhao, L., Liu, L., Liu, X., Shu, A., Zou, W., Wang, Z., Zhou, Y., Huang, C., Zhai, Y., He, H., 2024. Efficient phosphorus recovery from waste activated sludge: pretreatment with natural deep eutectic solvent and recovery as vivianite. Water Res. 263, 122161.